Desalination and Water Treatment
www.deswater.com
doi: 10.5004/dwt.2019.24618

167 (2019) 333–339
November

Experimental and mathematical modelling of cationic dye sorption in up-flow packed column using *Gracilaria corticata*

J. Thivya[a,*], J. Vijayaraghavan[b]

[a]*Department of Civil Engineering, University College of Engineering, Dindigul 624 622, Tamil Nadu, India, Tel. +91 94426 45058; emails: thivyaphd@gmail.com/thivyame@gmail.com*
[b]*Department of Civil Engineering, University College of Engineering, Ramanathapuram 623513, Tamil Nadu, India, Tel. +91 9488528279; email: vijayaraghavanmalar@gmail.com*

Received 26 February 2019; Accepted 24 June 2019

ABSTRACT

Herein, the biosorption capacity of red seaweed *Gracilaria corticata* towards cationic dye (crystal violet) in continuous mode of operation was evaluated. The experiments were conducted in a fixed column (up-flow) and the influence of flow rate and bed depth on dye removal was examined. Maximum dye uptake (49.5 mg/g) was obtained at the minimum flow rate (5 mL/min) and at the maximum bed depth (20 cm). The continuous experimental data, acquired from varying different parameters, were effectively modeled using the Yoon–Nelson, Thomas, and modified dose–response models. High accuracy was obtained in the calculated column breakthrough curves. The Yoon–Nelson and Thomas models were extremely accurate in predication of dye breakthrough curves, based on their correlation coefficients. The bed depth–service time model was also employed to predict breakthrough data. Regeneration of exhausted seaweed was possible using 0.01 M HCl as an elutant. After two sorption-elution cycles it was determined that *G. corticata* exhibited superior sorption capacities and % removal efficiencies.

Keywords: Water quality; Cationic dye; Red seaweed; Dye removal; Wastewater treatment

1. Introduction

The basic function of dyes, which are fundamentally chemical compounds, is to attach themselves to an array of surfaces and fabrics to convey colour [1]. It is this ability to impart colour that allows dyes to transcend many fields, which include the leather tanning industry [2,3], textile industry [4], food technology [5], paper production [6], paint industry [7], printing industry [8], light-harvesting arrays [9], agricultural research [10,11], hair colourings [12], and in photoelectrochemical cells [13]. This high demand for dyes has led to dye-production of 7×10^5–1×10^6 tons per year [14] with more than 100,000 different commercial dyes currently available. As with any high-production chemicals environmental issue may arise. Unfortunately, accurate mass of dyes discharged into the environment is unavailable. However, Hai et al. [15] has reported that approximately 10%–15% of dyes currently used to enter into the environment through wastes. The effect of dyes entered into our freshwater supply can have hazardous results. If 1 mg/L of dye is found in our fresh water sources it is unsuitable for human consumption. However, the effect on waters containing higher concentrations can be disastrous, halting the reoxygenation capacity of the receiving water as well as cutting off sunlight. This upsets the biological activity of the aquatic life within, including the photosynthetic capability of aquatic algae and plants [16–18]. Furthermore, dyes can be prepared from carcinogenetic precursors; hence, in general, dyes are carcinogenic and toxic, causing the dysfunction of kidneys, reproductive system, liver, the central nervous system and brain in humans [19].

* Corresponding author.

In order to combat these health and environmental issues several environmental protection agencies devised stringent regulations for dye-bearing wastewaters. This includes treatment of dye-bearing wastewater [20,21] prior to discharge and comply with minimum discharge limits of the treated water. However, stringent environmental regulations, forced numerous dye-based industries to implement green/environmentally friendly treatment strategies [22,23]. Two treatment techniques were generally employed: physico-chemical and biological methods. Physico-chemical involves ion-exchange, adsorption, precipitation, electrochemical and membrane technologies. However, these techniques bear many disadvantages [4,24], including cost, negative environmental impact and dependence on the wastes concentration. Hence the need is on the horizon for a more cost-efficient, eco-friendly method for wastewater treatment.

The removal of dyes using a passive biological technique, also known as biosorption, can be considered as a cheaper and more effective alternative [22,25]. This technique employs dead/inactive biomass for the removal of dyes. Biosorbents, the term given to the biological species used for dye-abstraction in wastewater, comprises of bacteria [4], fungi [26], algae [27] and polysaccharide materials [28]. Of these, marine algae are seldom utilized for the removal of dyes [29–31]. Our study employed *Gracilaria corticata*, a red marine alga, for the continuous abstraction of cationic dye (crystal violet (CV)) from aqueous solutions. In our previous batch equilibrium study the supreme biosorption capacity of *G. corticata* towards CV was highlighted [32]. The study elucidated the fundamental information regarding the biosorption efficiency and mechanism. However an examination using continuous column experiments will expose the technical feasibility of the technique under real scenarios [33]. Therefore, an up-flow packed column was used to conduct continuous-flow experiments based on various sorbent bed depths and solute flow rates. The continuous experimental data were described using several models and the sorbent was reactivated and used again to evaluate recycle potential.

2. Materials and methods

2.1. Preparation of the seaweed and chemical specifications

The red marine alga, *G. corticata*, was gathered from Mandapam (Tamilnadu, India) beaches. The collected seaweed was washed on site with deionized water followed by the drying process under sunlight. The dried seaweeds were then grounded to yield particles of 1.18 mm (average size) and subsequently employed for the research trials. All chemicals employed in this research were analytical grade and acquired from Sigma-Aldrich, India. The stock solution of dye (CV) was prepared by mixing CV (empirical formula = $C_{25}H_{30}N_3Cl$; molecular weight = 407.98 g/mmol) dye.

2.2. Continuous experiments

The glass column used for the continuous biosorption trails were 35 cm in length and had an internal diameter of 2 cm (Fig. 1). In order to vary the bed depth, a variable plunger was provided at the column top with a 0.5 mm stainless sieve. On the other hand, a 0.5 mm stainless sieve was present at the column bottom followed by glass wool. In order to maintain a consistent flow of the dye solution into the column, glass beads (1.5 mm in diameter) was positioned at height of 2 cm at the base of the column. Before the start of experiments, dried *G. corticata* seaweed was loaded in the column to achieve the required bed depth. In order to start the experiments, CV solution of desired concentration (100 mg/L, pH 8 and 30°C) was pumped upward at a fixed flow rate into the column with the aid of a peristaltic pump. The dye solution flow through the column and the samples exited the column at the top were examined for CV concentration using spectrophotometer (Spectroquant® Phara 300, Merck, Germany) at wavelength of 584 nm. The experiment was halted when the concentration of CV reached greater than 99.0 mg/L.

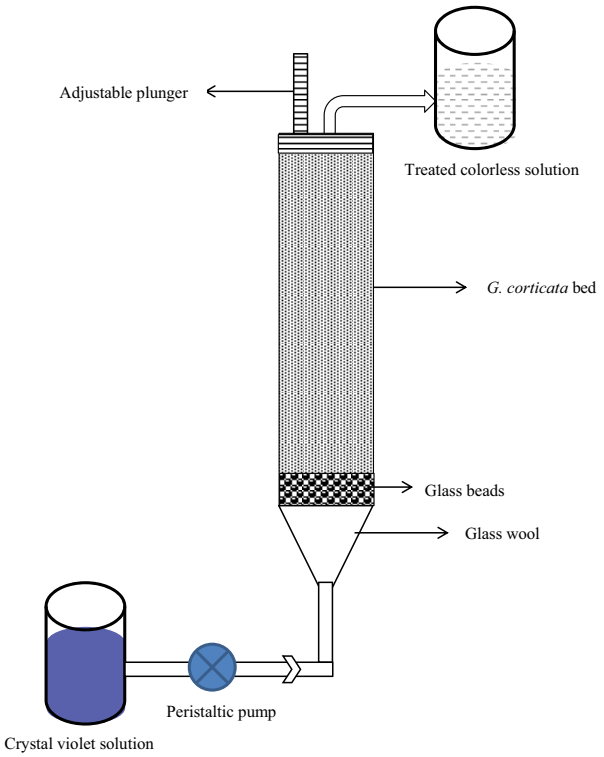

Fig. 1. Schematics of *G. corticata* loaded up-flow packed column.

The amount of dye remained in the column (m_{ad}) was estimated by multiplying the influent flow rate and the area above the breakthrough curve (C vs. t) [34]. The column sorptional uptake (Q) of the seaweed was calculated by dividing the dye mass (m_{ad}) by the mass of seaweed initially loaded in the column (M) [4].

The overall sorption zone (Δt) was estimated by subtracting column exhaustion time from the breakthrough time as follows [35]:

$$\Delta t = t_e - t_b \tag{1}$$

where t_e is the exhaustion time (min), the time at which CV concentration at the exit equals influent concentration and t_b is the breakthrough time (min), the time at which CV concentration at the exit reached 1 mg/L.

The effluent volume (V_{eff}) was determined as follows [36]:

$$V_{\text{eff}} = F \times t_e \tag{2}$$

where F is the volumetric flow rate (mL/min).

The overall quantity of CV molecules sent into the column (m_{total}) was determined as follows [36],

$$m_{\text{total}} = \frac{C_0 \times F \times t_e}{1,000} \tag{3}$$

The total percentage of CV removal was calculated as follows [37],

$$\text{Total dye removal}(\%) = \frac{m_{\text{ad}}}{m_{\text{total}}} \times 100 \tag{4}$$

The total CV mass eluted (m_d) was obtained from the elution curve (C vs. t), whereas the elution efficiency (E) was calculated as follows [4]:

$$E(\%) = \frac{m_d}{m_{\text{ad}}} \times 100 \tag{5}$$

All experiments were replicated twice; with the mean values of two replicate experiments being reported.

3. Results and discussion

3.1. Impact of bed depth on CV sorption

Using a continuous up-flow packed column the influence of column bed depth on the CV biosorption properties of *G. corticata* was examined. The bed depths examined were from 10 to 20 cm, whilst the inlet CV concentration and flow rate remained constant, at 100 mg/L and 5 mL/min, respectively. To achieve desired bed depths, 4.7, 6.1 and 8.1 g of *G. corticata* were loaded giving bed depths of 10, 15 and 20 cm, respectively. In all bed depths examined flat breakthrough curves were observed (Fig. 2). As bed depth increased which in turn increases the volume of binding sites, resulted in the elevation of the breakthrough and exhaustion times [38], generating a broadened sorption zone (Table 1). Due to the uptake capacity being very dependent on the amount of sorbent available, a correlation between the uptake capacity of *G. corticata* and the increase in bed depth was observed [39]. At 10, 15 and 20 cm bed depths, *G. corticata* exhibited CV uptake capacities of 41.3, 43.6 and 49.5 mg/g, respectively.

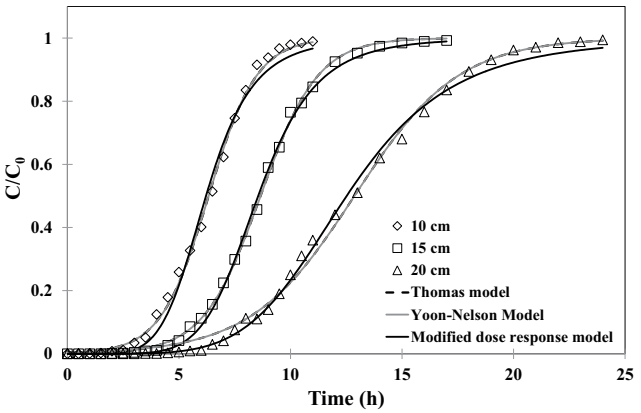

Fig. 2. Impact of bed depth on CV sorption capacity of *G. corticata*. The curves were predicted by different models. (Experimental conditions: flow rate = 5 mL/min; initial concentration of CV = 100 mg/L; pH = 8.0; temperature = 30°C).

By employing the bed depth-service time (BDST) model, the bed capacity at various breakthrough conditions can be physically predicted. The service time of the column was described as the time consumed by the concentration of CV to reach 1 mg/L. The BDST model's validity for CV-*G. corticata* system was determined by the linear plot obtained for bed depth vs. service time (Fig. not presented). Using the slope obtained from the BDST plot, the sorptional uptake of *G. corticata* per unit bed volume (N_0) was obtained assuming that linear velocity (υ) and initial concentration (C_0) were constant. From the intercept of BDST plot, the rate constant (K_a) was determined and it implies the solute transfer rate from the fluid to the solid phase [40]. The calculated N_0 was 2,528 mg/L, whereas K_a was found to be 0.042 L/mg h. The bed size was determined by K_a, if the value of K_a is high then only a small bed is sufficient to prevent breakthrough. However, as K_a declines it is necessary to elongate the bed to circumvent any breakthrough [40]. Interestingly, it is possible to scale up this process using the BDST model parameters without resorting to further experiments.

3.2. Impact of flow rate on CV sorption

The influence of flow rate on dye removal was examined as it has a major influence on biosorbent performance in continuous mode. For example, at elevated flow rates premature breakthrough and exhaustion were observed [36], due to a lack of solute residence time, in which a portion of the

Table 1
Column data and parameters obtained at different bed depths and flow rates during biosorption of CV onto *G. corticata*

Bed depth (cm)	Flow rate (mL/min)	CV uptake (mg/g)	t_b (h)	t_e (h)	Δt (h)	V_{eff} (L)	Total CV removal (%)
10	5	41.3	2.5	11.0	8.5	3.3	58.8
15	5	43.6	4.0	17.0	13.0	5.1	52.2
20	5	49.5	6.0	24.0	18.0	7.2	55.7
20	10	48.3	2.5	12.5	10.0	7.5	52.2
20	15	45.4	1.5	7.0	5.5	6.3	58.3

solute in the solution had not enough time to interact with the functional groups [30]. This is a vital factor when devising a biosorption packed column and fully utilizing the sorbent capacity. An increase in flow rates is also not efficient for intraparticle diffusion systems [41]. Furthermore, at very low flow rates external mass transfer will have an impact on the process [42].

For the present study, the flow rate was changed from 5 to 15 mL/min (Fig. 3). The initial CV concentration and bed depth were constant at 100 mg/L and 20 cm, respectively. High flow rates also had an influence on the biosorption potential of *G. corticata*, with depletion in CV uptake at higher flow rates being observed. At 5, 10 and 15 mL/min flow rates, *G. corticata* exhibited CV uptake capacities of 49.5, 48.3 and 45.4 mg/g, respectively. At higher flow rates, curtailed sorption zones and fairly sharp breakthrough curves were found; whereas the lowest flow rate yielded maximum column sorptional uptake (Table 1).

3.3. Column data modeling

In order to elucidate the column biosorption behavior of *G. corticata* at various bed depths and flow rates, several models were employed. These include,
Thomas model:

$$\frac{C_0}{C} = 1 + \exp\left(\frac{k_{TH}}{F}\left(Q_0 M - C_0 V_{eff}\right)\right) \tag{6}$$

Yoon-Nelson model:

$$\frac{C}{C_0} = \frac{\exp(k_{YN} t - \tau k_{YN})}{1 + \exp(k_{YN} t - \tau k_{YN})} \tag{7}$$

Modified dose-response model:

$$\frac{C}{C_0} = 1 - \frac{1}{1 + \left(\frac{V_{eff}}{b_{mdr}}\right)^{a_{mdr}}} \tag{8}$$

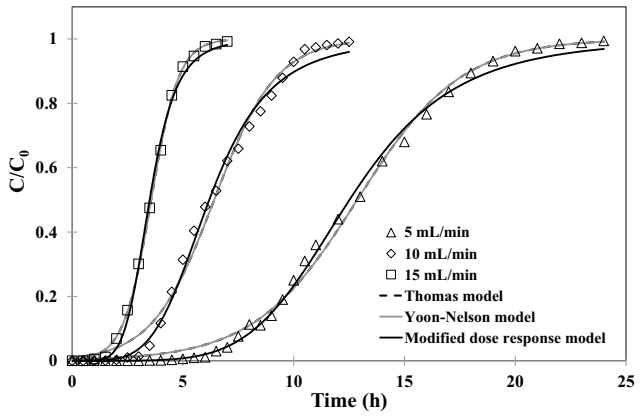

Fig. 3. Impact of flow rate on CV sorption capacity of *G. corticata*. The curves were predicted by different models. (Experimental conditions: bed height = 20 cm; initial concentration of CV = 100 mg/L; pH = 8.0; temperature = 30°C).

where Q_0 is the maximum sorption capacity of the seaweed (mg/g); k_{TH} is the rate constant of the Thomas model (L/mg h); V_{eff} is the volume of CV pumped into the column (L); τ is the Yoon-Nelson constant (min), which corresponds to time needed to attain 50% sorbate breakthrough; k_{YN} is the Yoon-Nelson model rate constant (1/min); a_{mdr} and b_{mdr} are the modified dose-response model constants. All the model parameters were evaluated by non-linear regression using Sigmaplot software.

The Thomas model is very popular for expressing column breakthrough data as it presumes Langmuir kinetics of sorption–desorption and no axial dispersion [43]. The Thomas model hypothesis is that sorption is the rate-determining step and follows reversible second-order reaction kinetics [36]. The two constants (k_{TH} and Q_0) of the Thomas model determined at various bed depths and flow rates are illustrated in Table 2. The values of the rate constant (k_{TH}) enhanced with decreasing bed depth and increasing flow rate. The rate constant describes the rate in which the solute is transferred from the liquid to the solid phase. On the other hand, a reverse trend was observed in the case of maximum solute uptake (Q_0). As predicted the values of Q_0 decreased with enhancing flow rate and declining bed depth values. This is basically due to the fact that high rate constants normally under-utilize the full sorption capacity of the seaweed. This could also be the result of intraparticle resistance. Furthermore, the Thomas model accurately calculated the experimental CV uptake values (Table 2), with the breakthrough curves been shown in Figs. 2 and 3.

The Yoon-Nelson model postulates that the decline in adsorption rate for each of the adsorbate is proportional to the probability of adsorbate sorption as well as the adsorbate breakthrough in the column [36]. The rate constant (k_{YN}) values are shown in Table 2, which exhibited identical trend as that of k_{TH} values. On the other hand, Yoon-Nelson model constant (τ) was found to be in good correlation with the experimental data at different bed depths and flow rates examined. As shown in Figs. 2 and 3, the curves determined by the Yoon-Nelson model correlates well with experimental breakthrough data.

In addition to the above models, the column biosorption data were also evaluated using the modified dose-response model. Yan et al. [44] developed and also suggested that the modified-dose response model eradicates the error caused by the Thomas model. This is particularly true at lower or higher time phases of the breakthrough curve. The constants (b_{mdr} and a_{mdr}) of the modified-dose response model are shown in Table 2. The calculated breakthrough curves obtained from the dose-response model at various bed depths and flow rates are shown in Figs. 2 and 3. Even with slightly inferior correlation coefficients than that of the Thomas and Yoon-Nelson models, the modified-dose response model reasonably predicted curves in good correlation with experimental data.

3.4. Regeneration

The recovery and subsequent reusability of biosorbents is paramount to its success in industrial applications, as it will ultimately reduce the constant dependency of the process on sorbent material as well as decrease the overall process costs and potential recovery of original solute [45]. Hence,

for a successful sorption process, it is expected to separate the adsorbed dye molecules from the sorbent and thereby regenerate the sorbent for subsequent usage. For the regeneration studies, about 8.1 g of *G. corticata* was initially loaded in the column to produce an initial bed depth of 20 cm. The inlet dye concentration was fixed at 100 mg/L, whereas flow rate was fixed at 5 mL/min. Table 3 lists the CV uptake, exhaustion time and breakthrough time observed during the two regeneration cycles examined. The breakthrough curves obtained during two CV sorption-elution cycles onto *G. corticata* are presented in Fig. 4. The first cycle column breakthrough was obtained at 6 h, whilst the sorption proceeds with column exhaustion at 24 h. The uptake capacity of *G. corticata* was calculated as 49.5 mg/g and removal efficiency as 55.7%.

At the end of the first cycle, the column was subjected immediately to the elution cycle using 0.01 M HCl as the elutant. Considering that sorption experiments were performed at alkaline conditions, the elution experiments were attempted at acidic solutions (0.01 M HCl). The elution curve obtained during the first regeneration cycle is presented in Fig. 4. By maintaining the flow rate of the elutant solution at 10 mL/min excessive elutant-biosorbent interaction was prevented. The elution curve for desorption of CV from CV-loaded *G. corticata* followed a common trend, in which a steep increase was found at the start of the process, after which a steady decrease was observed. The elutant exhibited excellent elution efficiency of 98%. As noted in Fig. 4, the elution process was completed within 4 h as compared to 24 h sorption cycle. This short elution process resulted in highly concentrated CV solutions in small volume of elutant. For example, the exit CV concentration was 1,278 mg/L after 30 min. The concentration factor, a method used to evaluate

Table 2
Thomas, Yoon–Nelson and modified dose–response model parameters at different bed depths and flow rates during biosorption of CV onto *G. corticata*

Bed depth (cm)	Flow rate (mL/min)	Thomas model			Yoon and Nelson model			Modified dose-response model			
		Q_0	k_{TH}	R^2	k_{YN}	τ	R^2	a_{mdr}	b_{mdr}	Q_0	R^2
10	5	40.4	0.0093	0.998	0.929	6.33	0.998	5.90	1.86	39.7	0.993
15	5	42.6	0.0078	0.999	0.778	8.66	0.999	6.58	2.57	42.1	0.998
20	5	47.7	0.0043	0.997	0.429	12.9	0.997	5.29	3.76	46.4	0.998
20	10	47.5	0.0072	0.992	0.992	6.41	0.997	4.51	3.71	45.8	0.995
20	15	39.6	0.016	0.999	1.60	3.57	0.999	5.73	3.15	38.8	0.998

Table 3
Sorption and elution process parameters for two sorption–elution cycles

Cycle number	CV uptake (mg/g)	t_b (h)	t_e (h)	Δt (h)	V_{eff} (L)	Total CV removal (%)	Time for elution (h)	Elution efficiency (%)	Concentration factor
1	49.5	6.0	24.0	18.0	7.2	55.7	4.0	98.0	6.0
2	46.3	5.0	22.0	17.0	6.6	55.4	3.5	98.7	6.3

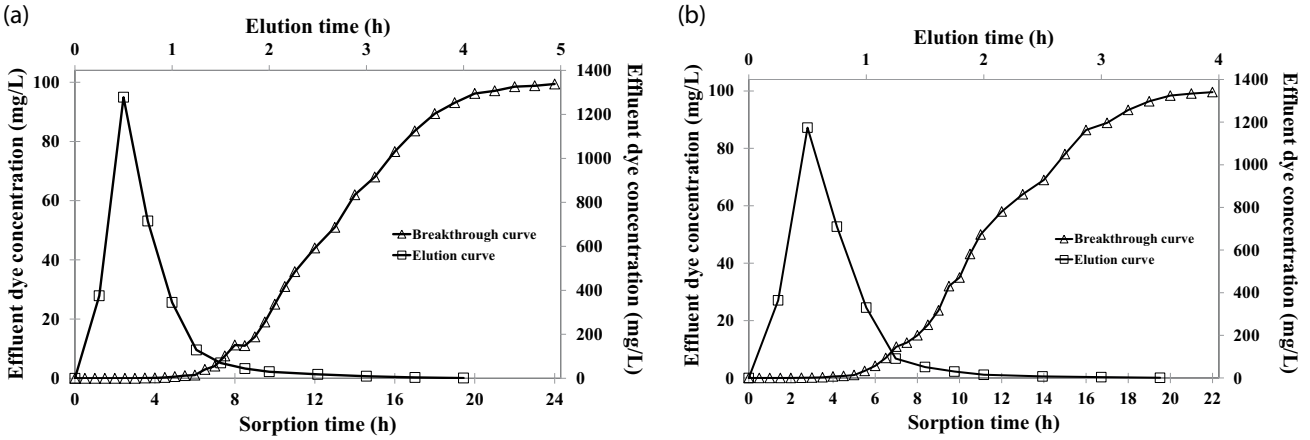

Fig. 4. Breakthrough and elution curves obtain during sorption of CV by *G. corticata* during two sorption-desorption cycles. (a) First cycle and (b) second cycle. (Experimental conditions: sorption flow rate = 5 mL/min; bed height = 20 cm; initial concentration of CV = 100 mg/L; sorption pH = 8.0; temperature = 30°C; elution flow rate = 10 mL/min).

the overall success of the biosorption process [46], for CV-*G. corticata* sorption-desorption process was determined as 6.0.

Once the elution process was completed, the column was washed carefully and continuously with deionized water until the exit wash solution was near pH 5.0. Fig. 4 shows breakthrough curve of CV onto *G. corticata* obtained during second sorption-elution cycle. Decreased breakthrough time and uptake values were obtained at the end of the second cycle, which shows a gradual breakdown of biomass due to continuous usage. Importantly, the decrease in uptake was only 6.5%, and this decrease loss of sorption performance may be because of blocked functional sites hindering the cycle's progress as well as due to acidic solutions used in the previous elution step. The elution step at the end of the second sorption cycle resulted in elution efficiency of 98.7% and the curve obtained is presented in Fig. 4.

4. Conclusions

In conclusion, our studies have shown that the red marine alga, *G. corticata*, is an effective and practical sorbent for the remediation of CV dye contaminated wastewater. Through continuous experiments, the impact of flow rate and bed depth on CV sorption was evaluated using an up-flow packed column. It was discovered that a decline in the flow rate favored biosorption, whilst an increase in the bed depth resulted in better column performance. At 20 cm bed depth and 5 mL/min flow rate, *G. corticata* bed portrayed 49.5 mg/g CV sorptional capacity. The implementation of the Yoon–Nelson, Thomas and modified dose–response models allowed for an adequate description of the experimental column data. Regeneration experiments for 2 cycles revealed possibility to recycle the seaweed with 0.01 M HCl as an elutant. A slight negative impact on biosorption performance was found as the cycles progressed; however, the red seaweed maintained consistently high CV uptakes greater than 46.3 mg/g. Thus, the present research highlights that *G. corticata* is a practical and efficient biosorbent for CV. These findings could be useful to implement biosorption technology for remediation of cationic-dye containing real wastewaters.

References

[1] M.T. Yagub, T.K. Sen, S. Afroze, H.M. Ang, Dye and its removal from aqueous solution by adsorption: a review, Adv. Colloid Interface Sci., 209 (2014) 172–184.
[2] O. Tünay, I. Kabdasli, D. Ohron, G. Cansever, Use and minimalization of water in leather tanning processes, Water Sci. Technol., 40 (1999) 237–244.
[3] H.R. Ong, D.M.R. Prasad, M.R. Khan, D.S. Rao, J. Nitthiyah, D.K. Raman, Effect of Jatropha seed oil meal and rubber seed oil meal as melamine urea formaldehyde adhesive extender on the bonding strength of plywood, J. Appl. Sci., 12 (2012) 1148–1153.
[4] K. Vijayaraghavan, Y.-S. Yun, Bacterial biosorbents and biosorption, Biotechnol. Adv., 26 (2008) 266–291.
[5] A. Slampova, D. Smela, A. Vondrackova, I. Jancarova, V. Kuban, Determination of synthetic colorants in foodstuffs, Chem. Listy, 95 (2001) 163–168.
[6] H. Liu, S. Yang, Y. Ni, Comparison of dye behavior from aspen HYP: dyes added in the HYP manufacturing process versus dyes added at the papermaking wet end, J. Wood Chem. Technol., 30 (2010) 118–128.
[7] M. Bohgard, A.-K. Ekholm, A method for the characterization of the aerosols emitted from handling of dye pigments in the paint manufacturing industry, J. Aerosol Sci., 21 (1990) S733–S736.
[8] G. Savvidis, E. Karanikas, N. Nikolaidis, I. Eleftheriadis, E. Tsatsaroni, Ink-jet printing of cotton with natural dyes, Color. Technol., 130 (2014) 200–204.
[9] R.W. Wagner, J.S. Lindsey, Boron-dipyrromethene dyes for incorporation in synthetic multi-pigment light-harvesting arrays, Pure Appl. Chem., 68 (1996) 1373–1380.
[10] S.M.F. Cook, D.R. Linden, Use of rhodamine WT to facilitate dilution and analysis of atrazine samples in short-term transport studies, J. Environ. Qual., 26 (1997) 1438–1441.
[11] H.R. Ong, M.R. Khan, A. Yousuf, N. Jeyaratnam, D.M.R. Prasad, Effect of waste rubber powder as filler for plywood application, Pol. J. Chem. Technol., 17 (2015) 41–47.
[12] T. Kojima, H. Yamada, T. Yamamoto, Y. Matsushita, K. Fukushima, Dyeing regions of oxidative hair dyes in human hair investigated by nanoscale secondary ion mass spectrometry, Colloids Surf., B, 106 (2013) 140–144.
[13] D. Wrobel, A. Boguta, R.M. Ion, Mixtures of synthetic organic dyes in a photoelectronic cell, J. Photochem. Photobiol., A, 138 (2001) 7–22.
[14] V.K. Gupta, Suhas, Application of low-cost adsorbents for dye removal – a review, J. Environ. Manage., 90 (2009) 2313–2342.
[15] F.I. Hai, K. Yamamoto, K. Fukushi, Hybrid treatment systems for dye wastewater, Crit. Rev. Env. Sci. Technol., 37 (2007) 315–377.
[16] C. Zaharia, D. Suteu, A. Muresan, R. Muresan, A. Popescu, Textile wastewater treatment by homogenous oxidation with hydrogen peroxide, Environ. Eng. Manage. J., 8 (2009) 1359–1369.
[17] S. Ramalingam, L. Parthiban, P. Rangasamy, Biosorption modeling with multilayer perceptron for removal of lead and zinc ions using crab shell particles, Arabian J. Sci. Eng., 39 (2014) 8465–8475.
[18] R. Senthilkumar, D. Aljoubory, Phenol degradation of industrial wastewater by photocatalysis, J. Innovative Eng., 2 (2014) 5.
[19] M.A.M. Salleh, D.K. Mahmoud, W.A.W.A. Karim, A. Idris, Cationic and anionic dye adsorption by agricultural solid wastes: A comprehensive review, Desalination, 280 (2011) 1–13.
[20] S. Kiran, A. Adeel, S. Kamal, M. Saeed, F.U. Rehman, T. Gulzar, Recent Trends and Future Prospects in Bioremediation of Synthetic Dyes: A Review, M. Yusuf, Ed., Handbook of Textile Effluent Remediation, Pan Stanford Publishing Pvt. Ltd., Singapore, 2018.
[21] M. Yusuf, A. Adeel, S. Kiran, M. Batool, M. Muneer, Insights into Dye Confiscation by Low-Cost Adsorbents for Textile Effluent Remediation: A Review, M. Yusuf, Ed., Handbook of Textile Effluent Remediation, Pan Stanford Publishing Pvt. Ltd., Singapore, 2018.
[22] K. Vijayaraghavan, R. Balasubramanian, Is biosorption suitable for decontamination of metal-bearing wastewaters? A critical review on the state-of-the-art of biosorption processes and future directions, J. Environ. Manage., 160 (2015) 283–296.
[23] S. Kiran, A. Adeel, S. Nosheen, M. Usman, M.A. Rafique, Recent Trends in Textile Effluent Treatments: A Review, Shahid-ul-Islam, Ed., Advanced Materials for Wastewater Treatment, Scrivener Publishing LLC, USA, 2017.
[24] E. Baranitharan, M.R. Khan, D.M.R. Prasad, Treatment of palm oil mill effluent in microbial fuel cell using polyacrylonitrile carbon felt as electrode, J. Med. Bioeng., 2 (2013) 252–256.
[25] N.K. Gupta, A. Sengupta, A. Gupta, J.R. Sonawane, H. Sahoo, Biosorption-an alternative method for nuclear waste management: a critical review, J. Environ. Chem. Eng., 6 (2018) 2159–2175.
[26] M.B. Asif, F.I. Hai, J. Hou, W.E. Price, L.D. Nghiem, Impact of wastewater derived dissolved interfering compounds on growth, enzymatic activity and trace organic contaminant removal of white rot fungi – a critical review, J. Environ. Manage., 201 (2017) 89–109.
[27] M. Sathishkumar, A. Mahadevan, K. Vijayaraghavan, S. Pavagadhi, R. Balasubramanian, Green recovery of gold through biosorption, biocrystallization, and pyro-crystallization, Ind. Eng. Chem. Res., 49 (2010) 7129–7135.

[28] G. Crini, Recent developments in polysaccharide-based materials used as adsorbents in wastewater treatment, Prog. Polym. Sci., 30 (2005) 38–70.
[29] R. Senthilkumar, D.M.R. Prasad, L. Govindarajan, K. Saravanakumar, B.S.N. Prasad, Green alga-mediated treatment process for removal of zinc from synthetic solution and industrial effluent, Environ. Technol., 40 (2019) 1262–1270.
[30] K. Vijayaraghavan, Y.-S. Yun, Competition of Reactive red 4, Reactive orange 16 and Basic blue 3 during biosorption of Reactive blue 4 by polysulfone-immobilized *Corynebacterium glutamicum*, J. Hazard. Mater., 153 (2008) 478–486.
[31] N. Mokhtar, E.A. Aziz, A. Aris, W.F.W. Ishak, N.S.M. Ali, Biosorption of azo-dye using marine macro-alga of *Euchema Spinosum*, J. Environ. Chem. Eng., 5 (2017) 5721–5731.
[32] J. Vijayaraghavan, T.B. Pushpa, S.J.S. Basha, K. Vijayaraghavan, J. Jegan, Removal of a basic dye from aqueous solution by *Gracilaria corticata*, J. Environ. Biotechnol. Res., 1 (2015) 30–36.
[33] K. Vijayaraghavan, F.D. Raja, Design and development of green roof substrate to improve runoff water quality: plant growth experiments and adsorption, Water Res., 63 (2014) 94–101.
[34] Z. Aksu, F. Gönen, Z. Demircan, Biosorption of chromium(VI) ions by Mowital®B30H resin immobilized activated sludge in a packed bed: comparison with granular activated carbon, Process Biochem., 38 (2002) 175–186.
[35] B. Volesky, J. Weber, J.M. Park, Continuous-flow metal biosorption in a regenerable *Sargassum* column, Water Res., 37 (2003) 297–306.
[36] Z. Aksu, F. Gönen, Biosorption of phenol by immobilized activated sludge in a continuous packed bed: prediction of breakthrough curves, Process Biochem., 39 (2004) 599–613.
[37] K. Vijayaraghavan, K. Palanivelu, M. Velan, Crab shell-based biosorption technology for the treatment of nickel-bearing electroplating industrial effluents, J. Hazard. Mater., 119 (2005) 251–254.
[38] C.A. Demarchi, A. Debrassi, J.D. Magro, N. Nedelko, A. Ślawska-Waniewska, P. Dłuzewski, J.-M. Greneche, C.A. Rodrigues, Adsorption of Cr(VI) on crosslinked chitosan–Fe(III) complex in fixed-bed systems, J. Water Process Eng., 7 (2015) 141–152.
[39] K. Vijayaraghavan, T. Ashokkumar, Plant-mediated biosynthesis of metallic nanoparticles: a review of literature, factors affecting synthesis, characterization techniques and applications, J. Environ. Chem. Eng., 5 (2017) 4866–4883.
[40] D.O. Cooney, Adsorption Design for Wastewater Treatment, CRC Press, Boca Raton, 1999.
[41] Z. Aksu, T. Kutsal, Determination of kinetic parameters in the biosorption of copper(II) on *Cladophora* sp., in a packed bed column reactor, Process Biochem., 33 (1998) 7–13.
[42] D.C.K. Ko, J.F. Porter, G. McKay, Optimised correlations for the fixed bed adsorption of metal ions on bone char, Chem. Eng. Sci., 55 (2000) 5819–5829.
[43] H.C. Thomas, Heterogeneous ion exchange in a flowing system, J. Am. Chem. Soc., 66 (1944) 1664–1666.
[44] G. Yan, T. Viraraghavan, M. Chen, A new model for heavy metal removal in a biosorption column, Adsorpt. Sci. Technol., 19 (2001) 25–43.
[45] K. Vijayaraghavan, M. Sathishkumar, R. Balasubramanian, Interaction of rare earth elements with a brown marine alga in multi-component solutions, Desalination, 265 (2011) 54–59.
[46] D.H.K. Reddy, K. Vijayaraghavan, J.A. Kim, Y.-S. Yun, Valorisation of post-sorption materials: opportunities, strategies, and challenges, Adv. Colloid Interface Sci., 242 (2017) 35–58.